

# Quasi-periodic oscillations during magnetar giant flares in the strangeon star model

Hong-Bo Li,<sup>1,2</sup> Yacheng Kang,<sup>1,2</sup> Zexin Hu,<sup>1,2</sup> Lijing Shao,<sup>2,3</sup>★ Cheng-Jun Xia,<sup>4</sup> and Ren-Xin Xu<sup>1,2</sup>†

<sup>1</sup>Department of Astronomy, School of Physics, Peking University, Beijing 100871, China

<sup>2</sup>Kavli Institute for Astronomy and Astrophysics, Peking University, Beijing 100871, China

<sup>3</sup>National Astronomical Observatories, Chinese Academy of Sciences, Beijing 100012, China

<sup>4</sup>Center for Gravitation and Cosmology, College of Physical Science and Technology, Yangzhou University, Yangzhou 225009, China

Accepted XXX. Received YYY; in original form ZZZ

## ABSTRACT

Soft gamma-ray repeaters (SGRs) are widely understood as slowly rotating isolated neutron stars. Their generally large spin-down rates, high magnetic fields, and strong outburst energies render them different from ordinary pulsars. In a few giant flares (GFs) and short bursts of SGRs, high-confidence quasi-periodic oscillations (QPOs) were observed. Although remaining an open question, many theoretical studies suggest that the torsional oscillations caused by starquakes could explain QPOs. Motivated by this scenario, we systematically investigate torsional oscillation frequencies based on the strangeon-star (SS) model with various values of harmonic indices and overtones. To characterize the strong-repulsive interaction at short distances and the non-relativistic nature of strangeons, a phenomenological Lennard-Jones model is adopted. We show that, attributing to the large shear modulus of SSs, our results explain well the high-frequency QPOs ( $\gtrsim 150$  Hz) during the GFs. The low-frequency QPOs ( $\lesssim 150$  Hz) can also be interpreted when the ocean-crust interface modes are included. We also discuss possible effects of the magnetic field on the torsional mode frequencies. Considering realistic models with general-relativistic corrections and magnetic fields, we further calculate torsional oscillation frequencies for quark stars. We show that it would be difficult for quark stars to explain all QPOs in GFs. Our work advances the understanding of the nature of QPOs and magnetar asteroseismology.

**Key words:** methods: numerical – stars: magnetars – stars: magnetic field – stars: oscillations

## 1 INTRODUCTION

Magnetars are the most highly magnetized neutron stars (NSs) in the Universe with typical magnetic fields  $B \gtrsim 10^{14}$  G. Judging from burst activities and other aspects, magnetars are classified into accretion-driven X-ray pulsars, X-ray bursters, anomalous X-ray pulsars (AXPs), soft gamma-ray repeaters (SGRs), etc. (Coelho & Malheiro 2014; Turolla et al. 2015). Among them, AXPs/SGRs are widely known as slowly rotating isolated NSs. Compared with ordinary pulsars, AXPs/SGRs usually have larger spin-down rates of  $\dot{P} \sim 10^{-13}$ – $10^{-10}$  s s<sup>-1</sup> with rotational periods in a narrower range of  $P \sim 2$ –12 s. In addition to persistent emissions and short bursts, giant flares (GFs) were observed associated with some SGRs. The peak luminosity during such GFs is  $10^6$  times greater than the Eddington luminosity of a typical NS (Mereghetti 2008; Huang & Yu 2014). These giant flares are typically accompanied by a decaying tail that lasts several hundred seconds. Some recorded GFs are as follows: SGR 0526–66 in 1979 (Mazets et al. 1979; Barat et al. 1983), SGR 1900+14 in 1998 (Hurley et al. 1999), SGR 1806–20 in 2004 (Terasawa et al. 2005; Palmer et al. 2005), SGR J1550–5418 in 2014 (Huppenkothen et al. 2014), SGR J1935+2154 in 2022 (Li et al. 2022b), and SGR 150228213 in 2023 (Chen et al. 2023).

With different timing analysis methods, many studies have revealed

the existence of characteristic quasi-periodic oscillations (QPOs) during these GFs. For different SGRs, the recorded QPOs are as follows: 43.5 Hz for SGR 0526–66 (Barat et al. 1983);  $18 \pm 2$  Hz,  $26 \pm 3$  Hz,  $30 \pm 4$  Hz,  $92 \pm 2$  Hz,  $150 \pm 17$  Hz,  $625 \pm 2$  Hz, and  $1837 \pm 5$  Hz for SGR 1806–20 (Israel et al. 2005; Watts & Strohmayer 2006; Strohmayer & Watts 2006);  $28 \pm 2$  Hz,  $53 \pm 5$  Hz, 84 Hz, and  $155 \pm 6$  Hz for SGR 1900+14 (Strohmayer & Watts 2005);  $93 \pm 12$  Hz,  $127 \pm 10$  Hz, and possibly 260 Hz for SGR J1550–5418 (Huppenkothen et al. 2014); 40 Hz for SGR J1935+2154 (Li et al. 2022b); 60 Hz and 110 Hz for SGR 150228213 (Chen et al. 2023). QPOs are also found in other phenomena. Some QPOs have been detected in gamma-ray bursts (GRBs): 22 Hz and 51 Hz for GRB 211211A (Xiao et al. 2022); 836 Hz, 1444 Hz, 2132 Hz, and 4250 Hz for GRB 200415A (Castro-Tirado et al. 2021); 0.0015 Hz for GRB 180620A (Zou & Liang 2022). Some QPOs are found in fast radio bursts (FRBs): 4.6 Hz for FRB 20191221A (Andersen et al. 2022); 2409 Hz for FRB 20201020A; 93.46 Hz for FRB 20210213A; 357.14 Hz for FRB 20210206A; 1052.63 Hz for FRB 20180916B A17; 588.24 Hz for FRB 20180916B A53 (Pastor-Marazuela et al. 2023).

Although the origin of QPOs remains uncertain, there are many theoretical studies on the nature of such events. Based on the ordinary NS scenarios, some models explore the idea that QPOs in some GFs are produced by the torsional oscillations of the solid crust alone or global seismic vibration modes (Duncan 1998; Piro 2005; Strohmayer & Watts 2005; Samuelsson & Andersson 2007; Sotani et al. 2007). However, not all observed frequencies can be explained

★ E-mail: lshao@pku.edu.cn (LS)

† E-mail: r.x.xu@pku.edu.cn (R-XX)

by these attempts. Considering the non-negligible effects of the high magnetic fields, superfluid, and nuclear pasta phases, there have been many investigations on the global oscillations of magnetars. (see [Glampedakis et al. 2006](#); [Levin 2006, 2007](#); [Cerdeira-Duran et al. 2009](#); [Colaiuda & Kokkotas 2011, 2012](#); [Colaiuda et al. 2009](#); [Gabler et al. 2011, 2012, 2013a,b, 2016, 2018](#); [van Hoven & Levin 2011, 2012](#); [Passamonti & Lander 2014](#), and references therein).

Alternatively, involving strange quark may shed light on the physical mechanism of the QPOs in GFs. It is conjectured that the bulk dense matter may be composed of strangeons, which are formerly named strange-quark clusters with nearly equal numbers of  $u$ ,  $d$ , and  $s$  quarks ([Xu 2003](#)). Based on phenomenological analysis and comparison with different observations, a strangeon star (SS) model was proposed with very stiff equation of states (EOSs; [Xu 2003](#); [Lai & Xu 2009](#)). Moreover, at realistic baryon densities of compact stars, the residual interaction between strangeons could be stronger than their kinetic energy, so strangeons would be trapped in the potential well and the bulk of the dense matter in the compact stars are crystallized into a solid state at low temperature ([Xu 2003, 2009](#)). SSs can account for many observational facts in astrophysics, such as pulsar glitches, sub-pulse driftings, extremely strong magnetic fields, the transient bursts of GCRT J1745–3009 (see e.g. [Xu et al. 1999](#); [Zhou et al. 2004](#); [Xu 2005](#); [Yue et al. 2006](#); [Zhu & Xu 2006](#); [Lai et al. 2023](#), for details), even for fast radio bursts related to Galactic magnetars ([Wang et al. 2022a,b](#)). To characterize the strong-repulsive interaction at short distances and the nonrelativistic nature of strangeons, a phenomenological Lennard-Jones model with two parameters has been adopted to describe the EOS of SSs ([Lai & Xu 2009](#)). Besides, the tidal deformability of merging binary SSs, as well as the ejecta and light curves, have been discussed by [Lai et al. \(2018, 2019, 2021\)](#). Recently, [Gao et al. \(2022\)](#) have discussed the universal relations between the moments of inertia, the tidal deformabilities, the quadrupole moments, and the shape eccentricity ([Gao et al. 2023](#)) of SSs.

If SSs indeed exist, they can release enough gravitational energy during starquakes to allow successful GFs to happen ([Xu et al. 2006](#); [Horvath 2007](#); [Xu 2007](#)). In other words, we can adopt the asteroseismological methods to probe the internal structure of compact stars. Some types of oscillation modes strongly couple to the space-time continuum, and can damp on relatively short time scales by emitting gravitational waves (GWs). [Li et al. \(2022a\)](#) have recently studied the oscillation modes and the related GWs of SSs. They discussed the universal relations between the fundamental ( $f$ )-mode frequencies and the global properties of SSs, such as compactness and tidal deformability. Moreover, inverted hybrid stars are discussed in [Zhang et al. \(2023\)](#), and extensions to pseudo-Newtonian gravity can be found in [Li et al. \(2023\)](#).

In the present work, for the first time we study the torsional oscillation modes of SSs in detail, and also discuss the effects of the magnetic field on the frequencies of the torsional modes. In the SS scenarios, we attempt to explain the observational QPO frequencies during the GFs of SGR 1806–20, SGR 1900+14 and SGR J1550–5418. Our results suggest that the SS-model can explain the high-frequency ( $\gtrsim 150$  Hz) QPOs, while it meets challenges of some low-frequency QPOs, such as the 18 Hz, 30 Hz and 92 Hz frequencies for SGR 1806–20, and the 40 Hz frequency for SGR J1935+2154. We attribute these difficulties to the large shear modulus of SSs, which could reach  $10^{32}$  erg cm $^{-3}$  ([Xu 2003](#)). In view of this, we further consider the interface modes of SSs in the interface between the ocean and crust to explain these low-frequency QPOs. Such an ocean layer could have a width in the range of  $\sim 10$ –50 m, consisting of a plasma of electrons and nuclei ([Medin & Cumming 2011](#)). The

Coulomb interaction energy between ions is greater than the thermal energy, leading to liquid behaviors. The ocean can influence the transport and release of thermal energy from the surface of SSs. It is in this ocean layer that the burning that produces X-ray bursts takes place. [McDermott et al. \(1988\)](#) have investigated non-radial oscillations of NSs with a fluid core, solid crust, and thin surface fluid ocean. Based on such a three-component model, they proposed a new oscillation mode called the interface mode. This interface mode can be caused by the interface not only between the ocean and the crust but also between the crust and the core. [Piro & Bildsten \(2005\)](#) have discussed the ocean-crust interface wave, exploring its properties both analytically and numerically for a two-component NS envelope model. We follow these ideas and apply them to SSs. We find that the ocean-crust interface mode of SSs can explain well the observed low-frequency QPOs in the GFs.

Furthermore, we also calculate the frequencies of the torsional modes of the quark stars (QSs), which were firstly proposed by [Witten \(1984\)](#). Typically, QSs could not have torsional shear modes due to its ultra-dense quark liquid extending up to the surface ([Haensel et al. 1986](#)). However, QSs can have a thin crust that extends to the neutron drip density ([Alcock et al. 1986](#)). [Jaikumar et al. \(2006\)](#) suggested that such a crust could be made up of nuggets of strange quark matter embedded in a uniform electron background. Although [Watts & Reddy \(2007\)](#) have calculated the torsional oscillations of QSs and discussed the effects of the magnetic field and temperature on the frequencies of torsional modes, their results should be modified using a more complete model with general-relativistic corrections and magnetic fields. We calculate the torsional oscillations for both the thin crust model and the quark nugget crust model in this work, and discuss the effects of the magnetic field on the frequencies.

The paper is organized as follows. In Sec. 2, we present our equilibrium models for SSs. For non-magnetized and magnetized stars, we discuss in Sec. 3 the numerical setups for solving the perturbation equations of the torsional oscillations with the Cowling approximation. In Sec. 4, we present the frequencies for SSs and QSs, as well as the fitting formulae for the effects of the magnetic field in the oscillation spectrum. Finally, we conclude in Sec. 5. Throughout this paper, we adopt geometric units with  $c = G = 1$ , where  $c$  and  $G$  are the speed of light and the gravitational constant, respectively.

## 2 EQUILIBRIUM CONFIGURATION

The general-relativistic equilibrium stellar model is assumed to be spherically symmetric and static, as described by the TOV equations. The line element of spacetime reads

$$ds^2 = -e^{2\Phi} dt^2 + e^{2\Lambda} dr^2 + r^2(d\theta^2 + \sin^2\theta d\phi^2), \quad (1)$$

where  $\Phi$  and  $\Lambda$  are functions of  $r$ . Typically, for magnetars, the magnetic energy ( $E_m$ ) is a few orders of magnitude smaller than the gravitational energy ( $E_g$ ) with a ratio,

$$\frac{E_m}{E_g} \sim \frac{B^2 R^3}{M^2/R} \sim 10^{-4} \left( \frac{B}{10^{16} \text{ G}} \right)^2, \quad (2)$$

where  $R$  and  $M$  are the radius and mass of a magnetar, respectively, and  $B$  is the surface magnetic field strength. In view of this, deformations on the spherical symmetry induced by the magnetic fields are usually small for magnetars ([Colaiuda et al. 2008](#); [Haskell et al. 2008](#)). Note that the general stress-energy tensor for a magnetized relativistic star is given by,

$$T^{\mu\nu} = (\rho + P)u^\mu u^\nu + P g^{\mu\nu} + H^2 u^\mu u^\nu + \frac{1}{2} H^2 g^{\mu\nu}, \quad (3)$$

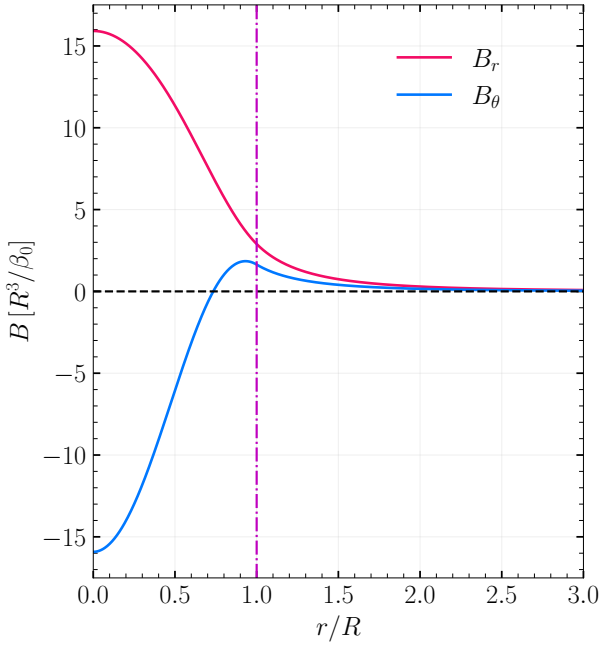


**Figure 1.** Profiles of the magnetic field components against the radial coordinate  $r$ .  $B_r$  and  $B_\theta$  are evaluated at  $\theta = 0$  and  $\theta = \pi/2$ , respectively. We set the compactness  $C = 0.2$ . The purple dotted-dashed line denotes the surface of the star.

where  $\rho$  is the energy density,  $P$  is the pressure,  $u^\mu$  is the 4-velocity of fluid, and  $H^\mu = B^\mu/\sqrt{4\pi}$  is the magnetic field.

Based on the above setting, Sotani et al. (2007) investigated torsional oscillations of relativistic stars with dipole magnetic fields. They showed that the magnetic field could exhibit a poloidal geometry, and can be derived by solving the Grad-Shafranov equation,

$$\frac{d^2 a_1}{dr^2} + (\Phi' - \Lambda') \frac{da_1}{dr} - \frac{2}{r^2} e^{2\Lambda} a_1 = -4\pi e^{2\Lambda} c_0 r^2 (\rho + P), \quad (4)$$

where  $a_1$  is the radial component of the electromagnetic four-potential, and  $c_0$  is a constant. We use primes to represent the radial derivatives hereafter. To solve Eq. (4), we must specify the boundary conditions at both the center and the surface of a star. Regularity of the solution at the origin requires  $a_1 = a_0 r^2$ , where  $a_0$  is a constant. At the surface, the internal solutions must be consistent with those above the surface with an external magnetic field. We consider a dipole field in the vacuum in this work. Therefore, the solution above the surface is given by,

$$a_1 = -\frac{3\beta_0}{8M^3} r^2 \left[ \ln \left( 1 - \frac{2M}{r} \right) + \frac{2M}{r} + \frac{2M^2}{r^2} \right], \quad (5)$$

where  $\beta_0$  is the magnetic dipole moment. The corresponding magnetic field thus has the form (Konno et al. 1999),

$$B_r = \frac{2 \cos \theta}{r^2} a_1, \quad (6)$$

$$B_\theta = -\frac{e^{-\Lambda} \sin \theta}{r} \frac{da_1}{dr}. \quad (7)$$

We plot in Fig. 1 the profiles of the magnetic field components,  $B_r$  and  $B_\theta$ , against the radial coordinate  $r$ . The magnetic fields are normalized by  $\beta_0/R^3$ . In this plot, we have used the polytropic EOS,  $P = k\rho^\gamma$ , with  $\gamma = 2$  and a compactness  $C = 0.2$  for the  $k$  value.

### 3 TORSIONAL OSCILLATIONS IN THE COWLING APPROXIMATION

Axial and polar perturbations do not couple with each other when we consider the pure axisymmetric perturbations on a spherically symmetric star. Here we consider only the torsional oscillations of a non-magnetized relativistic star with axial perturbations. The density variations in the spherically symmetric star would not be induced. For this reason, we neglect the perturbations of spacetime using the Cowling approximation. The axial perturbation equations for the elastic solid star in the Cowling approximation is written as (Samuelsson & Andersson 2007; Sotani et al. 2012),

$$Y'' + \left( \frac{4}{r} + \Phi' - \Lambda' + \frac{\mu'}{\mu} \right) Y' + \left[ \frac{\rho + P}{\mu} \omega^2 e^{-2\Phi} - \frac{(\ell+2)(\ell-1)}{r^2} \right] e^{2\Lambda} Y = 0, \quad (8)$$

where  $\mu$  is the shear modulus,  $\omega$  is the angular frequency,  $Y(r)$  describes the radial part of the angular oscillation amplitude, and the integer  $\ell$  is the angular separation constant which enters when  $Y(r)$  is expanded in spherical harmonics  $Y_{\ell m}(\theta, \phi)$ .

Now we extend our studies to the torsional oscillation of a magnetized relativistic star. Sotani et al. (2007) derived the perturbation equations of the magnetized relativistic star using the relativistic Cowling approximation. The final perturbation equation is,

$$A_\ell(r) Y'' + B_\ell(r) Y' + C_\ell(r) Y = 0, \quad (9)$$

where the coefficients are given in terms of the functions describing the equilibrium metric, fluid, and the magnetic field of the star,

$$A_\ell(r) = \mu + (1 + 2\lambda_1) \frac{a_1^2}{\pi r^4}, \quad (10)$$

$$B_\ell(r) = \left( \frac{4}{r} + \Phi' - \Lambda' \right) \mu + \mu' + (1 + 2\lambda_1) \frac{a_1}{\pi r^4} [(\Phi' - \Lambda') a_1 + 2a_1'], \quad (11)$$

$$C_\ell(r) = \left[ \left( \rho + P + (1 + 2\lambda_1) \frac{a_1^2}{\pi r^4} \right) e^{2\Lambda} - \frac{\lambda_1 a_1'^2}{2\pi r^2} \right] \omega^2 e^{-2\Phi} - (\lambda - 2) \left( \frac{\mu e^{2\Lambda}}{r^2} - \frac{\lambda_1 a_1'^2}{2\pi r^4} \right) + (2 + 5\lambda_1) \frac{a_1}{2\pi r^4} \{ (\Phi' - \Lambda') a_1' + a_1'' \}, \quad (12)$$

where  $\lambda = \ell(\ell + 1)$ , and  $\lambda_1 = -\ell(\ell + 1)/[(2\ell - 1)(2\ell + 3)]$ . To solve Eqs. (8) and (9) and determine the oscillation frequencies, the boundary conditions require that the traction vanishes at the top and the bottom of the crust. In the next section, we will use perturbation equations (8) and (9) to study torsional oscillation modes of the SSs and discuss possible effects from the magnetic field.

### 4 NUMERICAL RESULTS

We present results of torsional oscillation modes for SSs in Sec. 4.1, and make comparisons to QSs in Sec. 4.2.

#### 4.1 Strangeon stars

Xu (2003) conjectured that cold quark matter with very high baryon density could be in a solid state, and considered a SS at low temperature should be a solid star. The shear modulus of solid quark

**Table 1.** Frequencies (in the unit of Hz) of the fundamental torsional modes  ${}_{\ell}f_0$  for SSs without the magnetic fields (i.e.  $n = 0$  and  $B = 0$ ). The subscript in the models denote the SS mass; taking SS<sub>12</sub> as an example, the subscript “12” represents  $M = 1.2 M_{\odot}$ . Values in bold are close to the QPO observations (within 2%) for SGR 1806–20, SGR 1900+14 and SGR J1550–5418.

Model	$\ell = 2$	$\ell = 3$	$\ell = 4$	$\ell = 5$	$\ell = 6$	$\ell = 7$	$\ell = 8$	$\ell = 9$	$\ell = 10$
SS <sub>12</sub>	277	431.3	572.1	707.2	839.3	969.4	1098.3	1226.3	1353.6
SS <sub>14</sub>	<b>253.3</b>	394.9	524.2	648.6	770.2	890	1008.9	1126.9	1244.3
SS <sub>16</sub>	233	363.7	483.3	598.3	710.9	822.1	932.3	1041.8	1150.8
SS <sub>18</sub>	214.8	335.7	446.5	553.1	657.9	761.2	863.6	965.5	1067
SS <sub>20</sub>	198.4	310.4	413.3	512.5	609.9	706.1	801.5	896.4	991
SS <sub>22</sub>	183.5	287.5	383.2	475.6	566.3	656	745.1	833.7	922
SS <sub>24</sub>	169.7	<b>266.3</b>	355.4	441.5	526	609.7	692.8	775.5	858
SS <sub>26</sub>	<b>155.6</b>	244.6	326.7	406.2	484.4	561.7	<b>638.6</b>	715.1	791.4
SS <sub>28</sub>	<b>145</b>	228.1	305	379.5	452.7	525.2	597.2	668.9	740.3

**Table 2.** Same as Table 1, but for the first overtone ( $n = 1$ ) of the torsional modes  ${}_{\ell}f_1$  of SSs.

Model	$\ell = 2$	$\ell = 3$	$\ell = 4$	$\ell = 5$	$\ell = 6$	$\ell = 7$	$\ell = 8$	$\ell = 9$	$\ell = 10$
SS <sub>12</sub>	683.3	820.8	956.9	1090.6	1223	1354.3	1484.5	1614.3	1744.2
SS <sub>14</sub>	<b>612.3</b>	737.7	861	982.7	1103.4	1223.4	1342.7	1457.9	1579.8
SS <sub>16</sub>	551.5	666	778.8	890.4	1001.1	1111.2	1220.9	1330.1	1439.1
SS <sub>18</sub>	497.3	602	705.3	807.6	909.6	1010.9	1101.1	1212.6	1313.1
SS <sub>20</sub>	448.3	544.3	<b>639.1</b>	733.2	826.9	920.3	1013.4	1106.4	1193.3
SS <sub>22</sub>	404.3	492.2	579.3	666	752.4	838.6	924.6	1010.6	1096.5
SS <sub>24</sub>	363.9	444.5	524.5	604.2	683.8	763.4	842.9	922.5	1002
SS <sub>26</sub>	322.8	395.8	468.5	541.2	<b>613.9</b>	686.6	759.4	832.4	905.4
SS <sub>28</sub>	292.1	359.4	426.7	494	561.5	629	697	765	833.1

**Table 3.** Same as Table 1, but for the higher overtones  ${}_3f_n$  of the torsional modes of SSs for  $\ell = 3$ .

Model	$n = 2$	$n = 3$	$n = 4$	$n = 5$	$n = 6$	$n = 7$
SS <sub>12</sub>	820.8	1136.2	1434.4	1742.6	2042.2	2340.5
SS <sub>14</sub>	737.7	1016.6	1283.5	1558.2	<b>1821.2</b>	2091.5
SS <sub>16</sub>	665.9	916.3	1159.7	1400.7	1640.2	<b>1878.7</b>
SS <sub>18</sub>	602	825.7	1044	1260.2	1474.8	1689.1

matter could be  $\sim 10^{32}$  erg cm<sup>-3</sup> (Xu 2003), much larger than those of typical NSs ( $\sim 10^{30}$  erg cm<sup>-3</sup>; Duncan 1998; Piro 2005).

We first exhibit in Table 1 the frequencies of the SS fundamental modes  ${}_{\ell}f_0$  for  $\ell = 2$  to 10. It shows that the frequency of  $\ell = 2$  mode varies from 145 to 277 Hz, depending on the SS mass. Given the SS mass, the frequencies tend to increase with a higher  $\ell$ . In comparison, for NSs, the frequencies of the fundamental  $\ell = 2$  mode only range from 17 to 29 Hz (Sotani et al. 2007). Therefore, the frequency range of the  $\ell = 2$  mode of SSs is much larger than that of NSs. This is introduced by the larger shear modulus of SSs.

We show in Table 2 the frequencies of the first overtone  ${}_{\ell}f_1$  for

SSs. We find that the frequencies range from 300 Hz to 1700 Hz. Table 2 shows that the frequency of the first overtone decreases as the SS mass increases, which is the same as the fundamental modes in Table 1. However, such an anti-correlation differs from those of NSs, where the frequency of the first overtone would increase with a higher NS mass (Sotani et al. 2007). Note that such anti-correlation can also be found in higher overtones (see Table 3).

In order to compare with the torsional mode frequency of NSs, we calculate the torsional mode frequency of SSs using the same mass range of  $1.2M_{\odot}$ – $2.8M_{\odot}$ . However, the  $2.8M_{\odot}$  value is not the SSs’ maximum mass. As described in the Introduction, in a reasonable

model, the EOS of SSs is completely determined by the depth of the potential and the number density of baryons at the surface of the star. Because the strangeons are nonrelativistic there is a very strong repulsion at a short inter-cluster distance (Lai & Xu 2009, 2017; Gao et al. 2022; Li et al. 2022a), which could lead to the maximal mass of SSs over  $3 M_{\odot}$ .

In Tables 1, 2 and 3, we have marked the frequencies that are good fit (within 2%) to the observed QPO frequencies for some SGRs. For examples, we have: model SS<sub>26</sub> (whose  ${}_2f_0 = 155.6$  Hz) for SGR 1900+14, model SS<sub>24</sub> (whose  ${}_3f_0 = 266.3$  Hz) for SGR J1550–5418, and model SS<sub>14</sub> (whose  ${}_2f_1 = 612.3$  Hz) for SGR 1806–20. Based on our results, the observed high frequencies of 150 Hz, 625 Hz, and 1837 Hz might correspond to  ${}_2f_0$ ,  ${}_2f_1$ , and  ${}_3f_6$ , respectively. We also find that the SS model could explain well the high-frequency QPOs in the GFs of SGR 1806–20, SGR 1900+14 and SGR J1550–5418.

However, there appears to have difficulty when using the SS model to interpret the low-frequency QPOs (e.g., 18 Hz and 29 Hz for SGR 1806–20). For this reason, we propose that SSs may have a thin surface ocean with density and temperature in the range of  $10^6$ – $10^9$  g cm<sup>-3</sup> and  $10^8$ – $10^9$  K, respectively. With such an ocean layer, we can use the interface modes of the ocean-crust interface in order to explain the low-frequency QPOs. The frequency of the interface mode can be analytically approximated by (Piro & Bildsten 2005),

$$f \approx 16.5 \text{ Hz} \left( \frac{\Gamma}{173} \right)^{1/2} \left( \frac{T_8}{4} \right)^{1/2} \times \left( \frac{64}{A} \right)^{1/2} \left( \frac{10 \text{ km}}{R} \right) \left[ \frac{\ell(\ell+1)}{2} \right]^{1/2}, \quad (13)$$

where  $T_8 \equiv T/10^8$  K,  $A$  is the baryon number, and  $\Gamma$  is a dimensionless parameter that determines the liquid-solid transition via,

$$\Gamma \equiv \frac{(Ze)^2}{ak_B T} = \frac{127}{T_8/4} \left( \frac{Z}{30} \right)^2 \left( \frac{64}{A} \right)^{1/3} \left( \frac{\rho}{10^9 \text{ g cm}^{-3}} \right)^{1/3}, \quad (14)$$

where  $k_B$  is the Boltzmann's constant, and  $Z$  is the proton number. The crystallization point occurs at  $\Gamma = 173$  (Farouki & Hamaguchi 1993). Using Eq. (13), we calculate the frequencies of the interface modes with different  $\ell$ . The SS mass and radius are fixed at  $M = 1.4 M_{\odot}$  and  $R = 10$  km, respectively. According to Eq. (13), we see that the frequency is independent of the number of the overtone. It is not difficult to verify that the ocean-crust interface modes could interpret the recorded low-frequency QPOs, such as  ${}_1f = 16.3$  Hz,  ${}_2f = 28.5$  Hz, and  ${}_8f = 99$  Hz for SGR 1806–20,  ${}_4f = 52.1$  Hz and  ${}_7f = 87.3$  Hz for SGR 1900+14, and  ${}_3f = 40.4$  Hz for SGR J1935+2154.

As already emphasized by Sotani et al. (2007), the shift in the frequencies would be significant when the magnetic field exceeds  $\sim 10^{15}$  G. Following Sotani et al. (2007), now we discuss the effects of the magnetic fields. In the presence of magnetic fields, frequencies are shifted as,

$$\ell f_n = \ell f_n^{(0)} \left[ 1 + \ell \alpha_n \left( \frac{B}{B_{\mu}} \right)^2 \right]^{1/2}, \quad (15)$$

where  $\ell \alpha_n$  is a coefficient depending on the structure of the star, and  $\ell f_n^{(0)}$  is the frequency of the non-magnetized star. Note that the typical magnetic field strength is defined as  $B_{\mu} \equiv (4\pi\mu)^{1/2}$ . More details can be found in Messios et al. (2001).

In Figs. 2 and 3, we show the effects of the magnetic field on the frequencies of the torsional modes. The magnetic field strength is normalized by  $B_{\mu} = 4 \times 10^{16}$  G. Different dashed lines in Figs. 2 and 3 are our fits to the calculated numerical data with a high accuracy.

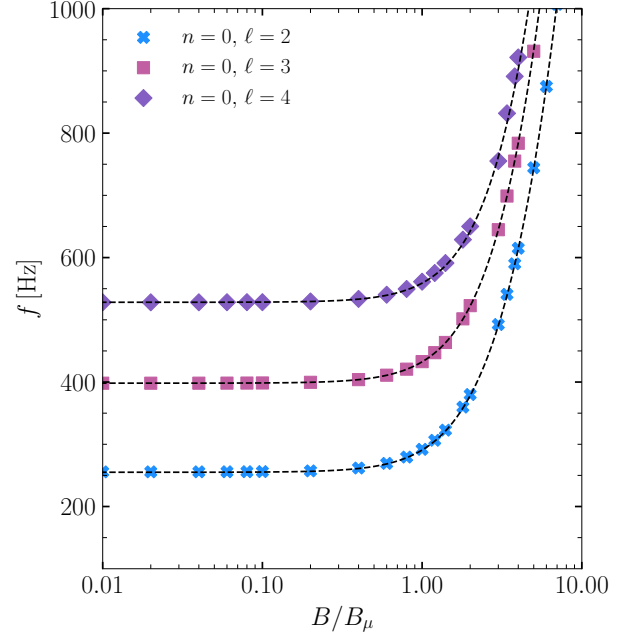


**Figure 2.** Frequencies of the fundamental  $n = 0$  modes with  $\ell = 2$ ,  $\ell = 3$ , and  $\ell = 4$  as a function of the magnetic field. We set the SS mass to be  $M = 1.4 M_{\odot}$ . Individual numerical results are denoted with different marks in different colours. The dashed lines correspond to the empirical formula (15) with different coefficient values. The fitting coefficients  $\ell \alpha_n$  are 0.3, 0.18, and 0.12 for  $\ell = 2$ ,  $\ell = 3$ , and  $\ell = 4$ , respectively.

For  $B > B_{\mu}$ , we find that the frequencies follow a quadratic increase against the magnetic field, and tend to become less sensitive to the SS parameters. NSs could have similar behaviors, but the turning-point value of the magnetic field strength is much lower ( $\sim 4 \times 10^{15}$  G; Sotani et al. 2007).

## 4.2 Comparisons with quark stars

The frequencies of torsional oscillations depend sensitively on the property of the crust. Considering there is no solid region for bare QSs, they could not account for the torsional shear oscillations. However, Alcock et al. (1986) suggested that QSs could have a thin nuclear crust that extends to the neutron drip density (i.e.  $\rho \approx 4 \times 10^{11}$  g cm<sup>-3</sup>). Jaikumar et al. (2006) proposed another possible model that a crust is made up of nuggets of strange quark matter embedded in a uniform electron background. In this subsection, we present detailed calculations of both models.

Following Watts & Reddy (2007), we use the standard general relativistic algorithm with a shear speed  $v_S = (\mu/\rho)^{1/2}$  and an alfvén speed  $v_A = B/(4\pi\rho)^{1/2}$ . We show in Fig. 4 the depth of the crust for different crust models.<sup>1</sup> We find that the shear speed in the nugget crust is smaller than that in the thin nuclear crust, which is consistent with the results at a constant pressure  $v_S \sim \sqrt{Z^{5/3}/A}$  in Watts & Reddy (2007), where  $A$  denotes the baryon number. In particular, Fig. 4 shows that both  $Z$  and  $Z/A$  of the nuggets decrease rapidly with the depth. In our calculation, for the thin nuclear crust models, the EOS of QSs is described by the MIT bag model, and the

<sup>1</sup> Note that the magnetic field is constant ( $B = 10^{14}$  G) in Fig. 4. When we discuss the effects of the magnetic field on the frequencies of torsional oscillations, we calculate the torsional oscillation frequencies using Eq. (9).

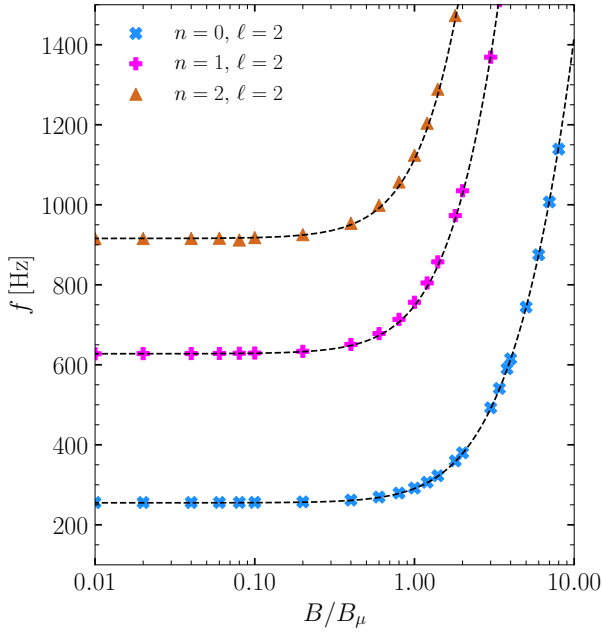


**Figure 3.** Frequencies of different overtones as a function of the normalized magnetic field for  $\ell = 2$ . The dashed lines are our fits using Eq. (15). The SS mass is  $M = 1.4 M_{\odot}$ . The coefficients  ${}_{\ell} \alpha_n$  are 0.3, 0.42 and 0.48 for  $n = 0$ ,  $n = 1$ , and  $n = 2$ , respectively.

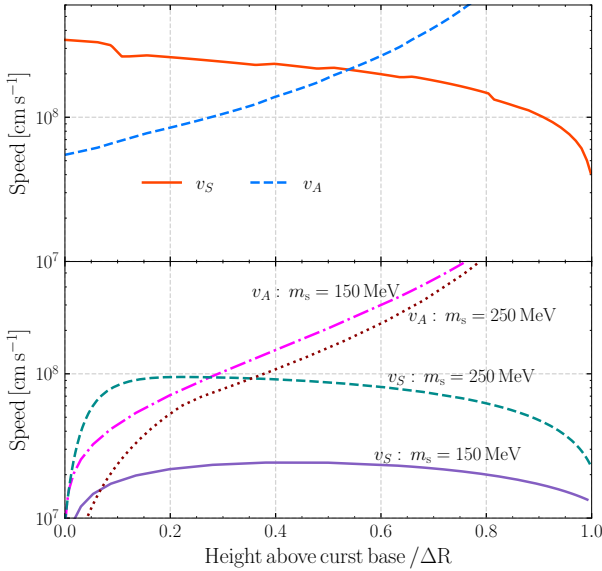


**Figure 4.** Shear speed  $v_S$  and Alfvén speed  $v_A$  in the crust of stars for a QS with a fixed mass  $M = 1.4 M_{\odot}$ , a radius  $R = 12$  km, and a magnetic field  $B = 10^{14}$  G. The upper panel is for the thin nuclear crust, and the lower panel is for the crust with nuggets. Note that in the lower panel, we consider  $m_s = 150$  MeV and  $m_s = 250$  MeV denoted with different lines in different colors.

EOS of the crust is given by Baym et al. (1971). The shear modulus  $\mu$  is,

$$\mu = 0.1194 \frac{n_i(Ze)^2}{a}, \quad (16)$$

where  $n_i$  is the ion number density,  $a = [3/(4\pi n_i)]^{1/3}$  is the average ion spacing, and  $+Ze$  is the ion charge.

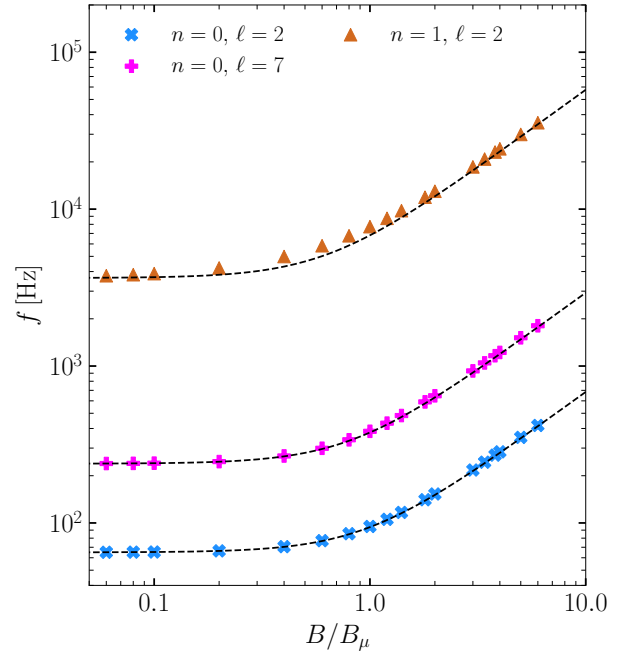


**Figure 5.** Torsional mode frequencies in the QS thin nuclear crust model as a function of the magnetic field. The dashed lines correspond to our fits using the empirical formula (15) with different coefficient values. The fitting values are 1.1, 1.5, and 2.5 for  ${}_2 f_0$ ,  ${}_7 f_0$ , and  ${}_2 f_1$ , respectively.

For the thin nuclear crust models, the frequency of the fundamental torsional mode with  $\ell = 2$ ,  ${}_2 f_0$ , is 64 Hz for a given mass  $M = 1.4 M_{\odot}$ . We find that the frequency of the fundamental torsional mode ranges from 26 to 64 Hz. To obtain a frequency  $\leq 30$  Hz requires a high mass ( $M \geq 2.4 M_{\odot}$  for all radii). The overtone frequencies are even higher for thin nuclear crust models. When  $B > B_{\mu} = 4 \times 10^{13}$  G the modes change the character and become dominated by the magnetic field.

In Fig. 5, we show the effects of the magnetic field on the torsional mode frequencies. The frequencies of the fundamental modes have increased by up to 35%, which is similar to NSs. The frequencies of the first overtone have increased by up to 24%. The typical value for magnetic field is  $B_{\mu} \equiv (4\pi\mu)^{1/2}$ , which depends on the crust EOS and the shear modulus. In particular, for the crust EOS that was described by Baym et al. (1971), the shear modulus could be  $\sim 10^{28}$  erg cm $^{-3}$ .

For the nugget crust models, we show in Fig. 6 the relations of the pressure and the shear modulus against energy density. Figure 6 shows that the EOS and shear modulus are sensitive to the strange quark mass,  $m_s$ . The number  $A$  and  $Z/A$  of nuggets decrease rapidly as the energy density increases. Using typical quark model parameters, i.e., the MIT bag constant  $B = 65$  MeV fm $^{-3}$  and  $m_s = 150$  MeV, we find that QSs can have a crust width of  $\Delta R = 40$  m for a given mass  $M = 1.4 M_{\odot}$  with a radius  $R = 10$  km. We find that the frequency of the fundamental mode and the first overtone is 5.11 Hz and 4282 Hz, respectively. Additionally, for  $m_s = 250$  MeV, we find that the thickness  $\Delta R$  is 217 m, and the frequency of the fundamental mode and the first overtone is 7.49 Hz and 2678 Hz, respectively. These results could explain some QPOs in the range of 18–150 Hz but it appears to be difficult to explain the high frequencies of 625 Hz and 1837 Hz.

In the left panel of Fig. 7, we show the relations between the torsional mode frequencies in the nugget crust model. We adopt

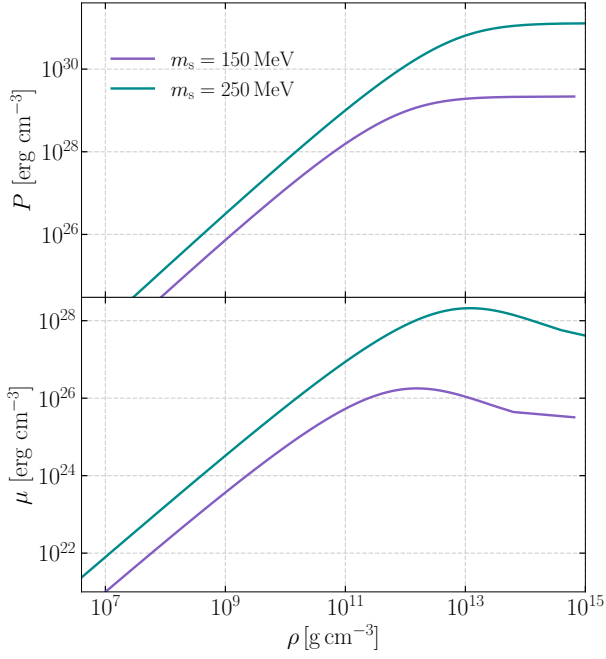


**Figure 6.** The upper panel shows the EOS of QSs in the nugget crust model. The lower panel shows the relationship between the shear modulus and the energy density.

$m_s = 150$  MeV and a normalized magnetic field  $B_\mu = 4 \times 10^{11}$  G. For this case when  $B = B_\mu$  the frequencies of fundamental mode have increased by up to 25%, compared to the frequencies of non-magnetized models. Using the empirical formula (15), we fit the coefficients for the effects of the magnetic field. The fitting coefficient values are 0.52, 0.49, and 0.07 for  ${}_2f_0$ ,  ${}_7f_0$ , and  ${}_2f_1$ , respectively. In the right panel of Fig. 7, we show the results with  $m_s = 250$  MeV and  $B_\mu = 4 \times 10^{14}$  G. The fitting coefficient values are 0.6, 2.3, and 5.6 for  ${}_2f_0$ ,  ${}_7f_0$ , and  ${}_2f_1$ , respectively. In both panels of Fig. 7, we find that, as expected, when the magnetic field strength is close to  $B_\mu = 4 \times 10^{14}$  G, the frequencies of the fundamental mode and the first overtone significantly increases.

Using a plane-parallel geometry, Watts & Reddy (2007) calculated the torsional oscillation of QSs, and discussed the effects of the magnetic field and temperature on the torsional mode frequencies. Similarly, in our work, we adopt the same EOS of the quark star and thin crust. However, the magnetic field is a constant in the work of Watts & Reddy (2007). Differently, we consider a relativistic star with dipole magnetic fields, calculate the frequencies of torsional modes, and study the effects of magnetic fields. Compared with earlier results, when considering the magnetic field strength  $B_\mu$ , the frequencies have increased by 25%–35% compared to the frequencies of non-magnetized models (see Figs. 5 and 7 in this paper and the left panels of Figs. 2 and 3 in Watts & Reddy 2007).

## 5 DISCUSSIONS AND CONCLUSIONS

In this work we first studied the torsional oscillation modes of SSs using the Cowing approximation with no magnetic field on the equilibrium configuration. According to our results, we find that SSs can explain well the high-frequency QPOs in the GFs of some SGRs. We further discuss the effects of magnetic field on the torsional oscillation frequencies. The typical value of the magnetic field strength is

adopted as  $B_\mu = 4 \times 10^{16}$  G, which is much larger than the ordinary NS models (Sotani et al. 2007).

To explain the observed low-frequency QPOs in the GFs of some SGRs, we consider that SSs may have a thin surface ocean with a density in the range of  $10^6$ – $10^9$  g cm $^{-3}$ . The depth is considered to be in the range of 10 – 50 m. We estimate the frequencies of the ocean-crust interface modes and find that the interface modes can interpret well the observed low-frequency QPOs in GFs for some SGRs.

Watts & Reddy (2007) have also investigated the thin nuclear crust model and the quark nugget crust model. They calculated the frequencies of the torsional oscillation modes using plane-parallel approximation and discussed the effects of the magnetic field and the temperature on the frequencies of the torsional modes. Compared with their results, when considering the magnetic field strength  $B_\mu$ , the frequencies have increased by up to 25%–35%, compared to the frequencies of non-magnetized models. For the thin nuclear crust model, the typical magnetic field value is  $B_\mu \sim 4 \times 10^{13}$  G. The frequencies of the first overtone could increase up to 24% at  $B_\mu \sim 4 \times 10^{13}$  G. The nugget crust model has a wider range of frequencies due to its uncertainty in the strange quark mass  $m_s$ . Our results show that both the thin nuclear crust model and the nugget crust model are difficult to reproduce well the recorded QPO frequencies.

Analysis of the magnetar QPOs in GFs could enable us to look for a correct interpretation of their origin and the physical nature of the oscillations (Abbott et al. 2009; Kalmus et al. 2009; Abadie et al. 2011; Abbott et al. 2022). In the future, the strong couplings of magnetar oscillations to GWs will provide an excellent opportunity to apply the asteroseismological methods to compact star studies, and eventually uncover the nature of astrophysical compact objects.

## ACKNOWLEDGEMENTS

We thank the anonymous referee for comments. This work was supported by the National SKA Program of China (2020SKA0120300, 2020SKA0120100), the National Natural Science Foundation of China (11975027, 11991053, 12275234, 12342027), the Max Planck Partner Group Program funded by the Max Planck Society, and the High-Performance Computing Platform of Peking University.

## DATA AVAILABILITY

The data underlying this paper will be shared on reasonable request to the corresponding authors.

## REFERENCES

- Abadie J., et al., 2011, *ApJL*, 734, L35
- Abbott B. P., et al., 2009, *ApJ*, 701, L68
- Abbott R., et al., 2022, *arXiv e-prints*, p. arXiv:2210.10931
- Alcock C., Farhi E., Olinto A., 1986, *ApJ*, 310, 261
- Andersen B. C., et al., 2022, *Nature*, 607, 256
- Barat C., et al., 1983, *A&A*, 126, 400
- Baym G., Pethick C., Sutherland P., 1971, *ApJ*, 170, 299
- Castro-Tirado A. J., et al., 2021, *Nature*, 600, 621
- Cerda-Duran P., Stergioulas N., Font J. A., 2009, *MNRAS*, 397, 1607
- Chen R.-C., Deng C.-M., Wang X.-G., Zhou Z.-M., Yang X., Lin D.-B., Wang Q., Liang E.-W., 2023, *RAA*, 23, 085018
- Coelho J. G., Malheiro M., 2014, *Publ. Astron. Soc. Jap.*, 66, 14
- Colaiuda A., Kokkotas K. D., 2011, *MNRAS*, 414, 3014
- Colaiuda A., Kokkotas K. D., 2012, *MNRAS*, 423, 811

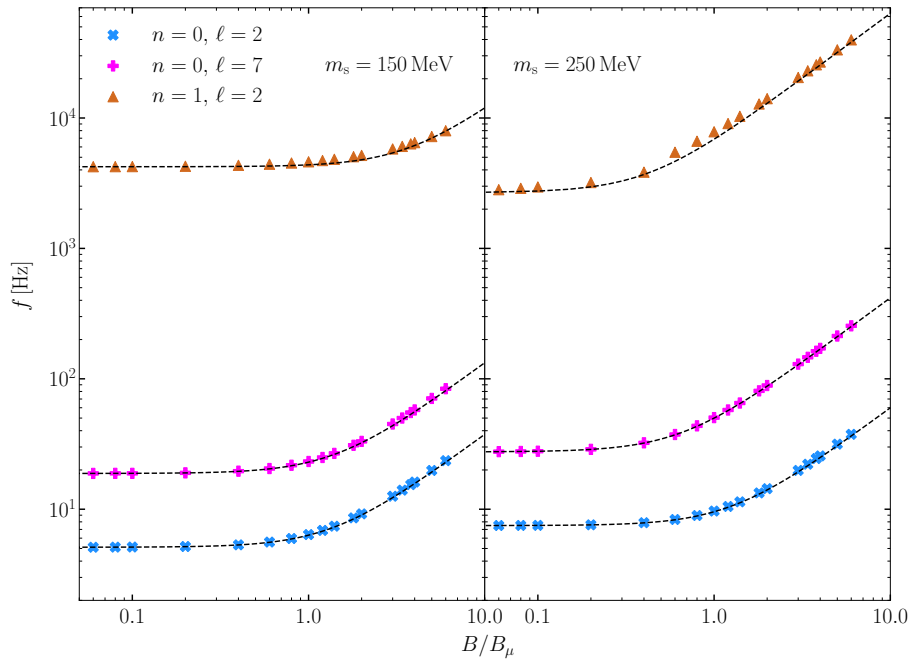


**Figure 7.** Frequencies of the fundamental  $n = 0$  modes with  $\ell = 2, 7$  and the first overtone in the nugget crust model. The left panel shows the results with strange quark mass  $m_s = 150$  MeV and the normalized magnetic field strength  $B_\mu = 4 \times 10^{11}$  G, while for the right panel  $m_s = 250$  MeV and  $B_\mu = 4 \times 10^{14}$  G. The lines correspond to our fits using the empirical formula (15) with different coefficient values.

- Colaiuda A., Ferrari V., Gualtieri L., Pons J. A., 2008, *MNRAS*, 385, 2080  
Colaiuda A., Beyer H., Kokkotas K. D., 2009, *MNRAS*, 396, 1441  
Duncan R. C., 1998, *ApJ*, 498, L45  
Farouki R. T., Hamaguchi S., 1993, *Phys. Rev. E*, 47, 4330  
Gabler M., Cerda-Duran P., Font J. A., Muller E., Stergioulas N., 2011, *MNRAS*, 410, 37  
Gabler M., Duran P. C., Stergioulas N., Font J. A., Muller E., 2012, *MNRAS*, 421, 2054  
Gabler M., Cerda-Durán P., Stergioulas N., Font J. A., Muller E., 2013a, *Phys. Rev. Lett.*, 111, 211102  
Gabler M., Cerda-Duran P., Font J. A., Muller E., Stergioulas N., 2013b, *MNRAS*, 430, 1811  
Gabler M., Cerda-Durán P., Stergioulas N., Font J. A., Muller E., 2016, *MNRAS*, 460, 4242  
Gabler M., Cerda-Durán P., Stergioulas N., Font J. A., Muller E., 2018, *MNRAS*, 476, 4199  
Gao Y., Lai X. Y., Shao L., Xu R. X., 2022, *MNRAS*, 509, 2758  
Gao Y., Shao L., Steinhoff J., 2023, *ApJ*, 954, 16  
Glampedakis K., Samuelsson L., Andersson N., 2006, *MNRAS*, 371, L74  
Haensel P., Zdunik J. L., Schaefer R., 1986, *A&A*, 160, 121  
Haskell B., Samuelsson L., Glampedakis K., Andersson N., 2008, *MNRAS*, 385, 531  
Horvath J. E., 2007, *Astrophys. Space Sci.*, 308, 431  
Huang L., Yu C., 2014, *ApJ*, 796, 3  
Huppenkothen D., et al., 2014, *ApJ*, 787, 128  
Hurley K., et al., 1999, *Nature*, 397, 41  
Israel G., et al., 2005, *ApJ*, 628, L53  
Jaikumar P., Reddy S., Steiner A. W., 2006, *Phys. Rev. Lett.*, 96, 041101  
Kalmus P., Cannon K. C., Marka S., Owen B. J., 2009, *Phys. Rev. D*, 80, 042001  
Konno K., Obata T., Kojima Y., 1999, *A&A*, 352, 211  
Lai X. Y., Xu R. X., 2009, *MNRAS*, 398, 31  
Lai X. Y., Xu R. X., 2017, *J. Phys. Conf. Ser.*, 861, 012027  
Lai X. Y., Yu Y. W., Zhou E. P., Li Y. Y., Xu R. X., 2018, *RAA*, 18, 024  
Lai X. Y., Zhou E. P., Xu R. X., 2019, *Eur. Phys. J. A*, 55, 60  
Lai X. Y., Xia C. J., Yu Y. W., Xu R. X., 2021, *RAA*, 21, 250  
Lai X., Xia C., Xu R., 2023, *Advances in Physics X*, 8, 2137433  
Levin Y., 2006, *MNRAS*, 368, L35  
Levin Y., 2007, *MNRAS*, 377, 159  
Li H.-B., Gao Y., Shao L., Xu R.-X., Xu R., 2022a, *MNRAS*, 516, 6172  
Li X., et al., 2022b, *ApJ*, 931, 56  
Li H.-B., Gao Y., Shao L., Xu R., Xu R.-X., 2023, *Phys. Rev. D*, 108, 064005  
Mazets E. P., Golenetskii S. V., Il'inskiy V. N., Aptekar' R. L., Guryan Y. A., 1979, *Nature*, 282, 587  
McDermott P. N., van Horn H. M., Hansen C. J., 1988, *ApJ*, 325, 725  
Medin Z., Cumming A., 2011, *ApJ*, 730, 97  
Mereghetti S., 2008, *Astron. Astrophys. Rev.*, 15, 225  
Messios N., Papadopoulos D. B., Stergioulas N., 2001, *MNRAS*, 328, 1161  
Palmer D. M., et al., 2005, *Nature*, 434, 1107  
Passamonti A., Lander S. K., 2014, *MNRAS*, 438, 156  
Pastor-Marazuela I., et al., 2023, *A&A*, 678, A149  
Piro A. L., 2005, *ApJ*, 634, L153  
Piro A. L., Bildsten L., 2005, *ApJ*, 619, 1054  
Samuelsson L., Andersson N., 2007, *MNRAS*, 374, 256  
Sotani H., Kokkotas K. D., Stergioulas N., 2007, *MNRAS*, 375, 261  
Sotani H., Nakazato K., Iida K., Oyamatsu K., 2012, *Phys. Rev. Lett.*, 108, 201101  
Strohmayer T. E., Watts A. L., 2005, *ApJ*, 632, L111  
Strohmayer T. E., Watts A. L., 2006, *ApJ*, 653, 593  
Terasawa T., et al., 2005, *Nature*, 434, 1110  
Turolla R., Zane S., Watts A., 2015, *Rept. Prog. Phys.*, 78, 116901  
Wang W.-Y., Jiang J.-C., Lu J., Xu H., Xu J., Lee K., Liu J., Xu R., 2022a, *Science China Physics, Mechanics, and Astronomy*, 65, 289511  
Wang W.-Y., Yang Y.-P., Niu C.-H., Xu R., Zhang B., 2022b, *ApJ*, 927, 105  
Watts A. L., Reddy S., 2007, *MNRAS*, 379, L63  
Watts A. L., Strohmayer T. E., 2006, *ApJ*, 637, L117  
Witten E., 1984, *Phys. Rev. D*, 30, 272  
Xiao S., et al., 2022, *arXiv e-prints*, p. arXiv:2205.02186  
Xu R.-X., 2003, *ApJ*, 596, L59  
Xu R. X., 2005, *MNRAS*, 356, 359  
Xu R.-X., 2007, *Adv. Space Res.*, 40, 1453  
Xu R., 2009, *J. Phys. G*, 36, 064010  
Xu R. X., Qiao G. J., Zhang B., 1999, *ApJ*, 522, L109  
Xu R.-X., Tao D. J., Yang Y., 2006, *MNRAS*, 373, L85



- Yue Y.-L., Cui X. H., Xu R. X., 2006, *ApJ*, 649, L95  
Zhang C., Luo Y., Li H.-b., Shao L., Xu R., 2023, *arXiv e-prints*, p. [arXiv:2306.08234](https://arxiv.org/abs/2306.08234)  
Zhou A. Z., Xu R.-X., Wu X. J., Wang N., Hong X. Y., 2004, *Astropart. Phys.*, 22, 73  
Zhu W. W., Xu R.-X., 2006, *MNRAS*, 365, L16  
Zou L., Liang E.-W., 2022, *MNRAS*, 513, L89  
van Hoven M., Levin Y., 2011, *MNRAS*, 410, 1036  
van Hoven M., Levin Y., 2012, *MNRAS*, 420, 3035

This paper has been typeset from a  $\text{\TeX/L\TeX}$  file prepared by the author.